Highlights

Retrofit Electromagnetic Shielding of CSST to Mitigate Fires from Lightning Transients, AC Fault Currents, and Ground Potential Rise

Ramanathan Karthikeyan

- Three distinct arc failure modes identified in bonded CSST installations; bonding mandate exacerbates two of the three.
- Ungrounded roof fastener array identified as the principal proposed arc source and a gap in existing research literature.
- Retrofit electromagnetic shielding demonstrated as the only measure resolving all three failure modes simultaneously.
- Shield continuity is directly field-verifiable by resistance measurement — unique among all current CSST protection measures.

Retrofit Electromagnetic Shielding of CSST to Mitigate Fires from Lightning Transients, AC Fault Currents, and Ground Potential Rise

Ramanathan Karthikeyan[a,*]

[a]PyroThor LLC, Sheridan, WY, 82801, USA

ARTICLE INFO

Keywords:
Corrugated stainless steel tubing
CSST
electromagnetic shielding
Faraday cage
lightning fire
ground potential rise
action integral
arc perforation
retrofit shielding
corona discharge
coaxial cable analogy
fire safety engineering

ABSTRACT

Corrugated Stainless Steel Tubing (CSST), installed in an estimated 6 to 12 million American homes since 1988, represents a systematically underreported residential fire hazard. The thin CSST wall (0.15–0.25 mm) renders it acutely vulnerable to arc perforation by lightning-induced transients. The industry's primary regulatory response — bonding CSST to the building's electrical grounding system per ICC IFGC §310.2 — is demonstrated to be physically counterproductive. It communicates Ground Potential Rise (GPR) to the gas tube while leaving the principal proposed arc source unaddressed: an ungrounded array of metallic roof fasteners that accumulate charge toward cloud potential through electrostatic induction, behaving as distributed corona electrodes above the CSST runs below. Drawing on Gauss's Law, Maxwell's equations, the coaxial cable shielding analogy, and laboratory perforation testing, this paper develops a physical framework establishing that retrofit electromagnetic shielding — a continuous external conductive enclosure applied from manifold to appliance terminus — is the only engineering measure that simultaneously resolves all three identified arc failure modes: lightning-induced arc initiation from the roof fastener array; GPR-driven jacket breakdown communicated through the bonding connection; and 60 Hz AC fault current arcing from household wiring in shared spaces. Because the retrofit shield intercepts external electromagnetic energy on its outer surface while isolating the gas tube within, it renders the bonding mandate unnecessary and provides the highest degree of protection achievable against the full spectrum of identified arc hazards — a universality of coverage no currently deployed single measure, including arc-resistant CSST products and the bonding mandate itself, can match.

1. Introduction

Corrugated Stainless Steel Tubing (CSST) was introduced into the United States residential gas distribution market in approximately 1988 as a seismic-resilient, labor-saving alternative to Schedule 40 black iron pipe. CSST has been installed in at least seven million American homes comprising over one billion feet of gas piping as of 2012 [1], with contemporary estimates projecting an installed base of 1.5 to 2 billion linear feet across 12 to 17 million structures. Its defining structural feature — a thin corrugated stainless steel wall of 0.15 to 0.25 mm — renders it susceptible to arc perforation by lightning-induced electromagnetic transients, as established in published laboratory testing and fire investigations [2, 3, 4, 5]. The industry's primary regulatory response — mandated bonding of CSST to the building's electrical grounding system under ICC IFGC §310.2 and IRC G2411.2 — is demonstrated in this paper to be physically counterproductive. It fails to address the principal proposed arc source (the ungrounded roof fastener array at cloud potential, discussed in Section 3.2) and introduces a secondary failure mechanism, Ground Potential Rise, that increases arc risk in high-energy lightning events. This paper presents retrofit electromagnetic shielding as the only engineering solution consistent with the physics of the hazard.

A structural limitation in national fire data collection compounds the public safety dimension of this hazard. The National Fire Incident Reporting System (NFIRS) contains no dedicated cause-of-ignition field for CSST, meaning that CSST-attributable lightning fires are recorded under generic lightning or electrical cause codes [1]. This absence of CSST-specific incident data prevents systematic analysis of the hazard and makes it impossible to assess whether installed mitigation measures are producing measurable reductions in fire incidence — a limitation explicitly identified by the Fire Protection Research Foundation's Phase 1 investigation in 2011, which recommended CSST be added as a dedicated NFIRS category [27]. The practical consequence is that documented incidents, including the line-of-duty deaths of Lieutenant Nathan Flynn (Howard County, MD, 2018) and Battalion Chief Joshua Laird (Frederick County, MD, 2021) — both formally attributed to lightning-induced CSST arc failure by the ATF [12] — occurred in an environment where the national fire data infrastructure lacked the resolution to identify a pattern from prior events.

This paper makes four principal contributions: (1) a quantitative perforation failure analysis based on the action integral framework; (2) an analysis of the ungrounded roof electrode array as the principal proposed arc source, incorporating electrostatic corona discharge physics; (3) a rigorous critique of the ICC bonding mandate based on Ground Potential Rise physics, with reference to peer-reviewed experimental documentation (Saba et al. [6]); and (4) a formal development of the retrofit electromagnetic shielding solution using Gauss's Law and the coaxial cable analogy.

Scope and Limitation: This paper is limited to the theoretical development of retrofit electromagnetic shielding as a solution to the CSST lightning fire hazard. The analysis is grounded in fundamental electromagnetic principles —

*Corresponding author
Email address: admin@pyrothor.com (R. Karthikeyan)
ORCID(s):

Gauss's Law, Maxwell's equations, and the coaxial cable analogy — and does not extend to experimental validation of any specific commercial implementation. The paper offers a design specification and a theoretical argument; experimental confirmation and code adoption are left for subsequent investigation.

2. Background: Physical Basis of CSST Arc Perforation

2.1. Material and Geometric Properties of CSST

CSST consists of a corrugated 304-grade stainless steel tube with wall thickness of 0.15 to 0.25 mm, enclosed within a polyethylene (PE) outer jacket of approximately 1 mm thickness. The corrugated geometry provides mechanical flexibility and accommodates seismic movement. For electromagnetic analysis, the corrugated metallic geometry is significant: the corrugated stainless steel tube exhibits inductive and capacitive properties consistent with a distributed transmission line, and its geometric resemblance to helical conductors used in RF antenna loading coils is not coincidental — both are efficient RF current-carrying geometries. CSST is, in this sense, a radio frequency conductor first, adapted for gas transport.

The Interscience Communications technical report [4] on CSST arc perforation identified two critical physical properties that define the vulnerability: (1) the wall thickness is so small that only localized heating and arc attachment — not mechanical stress — is required to cause perforation; and (2) the failure is highly localized, consistent with the attachment of a high-current arc to a small area of the stainless steel surface. Arc attachment melts a region of the wall typically 1 to 3 mm in diameter, ejects the molten material, and leaves a characteristic hole with resolidified metal around the rim. This mechanism is observed consistently across laboratory samples and forensic field samples [3, 4, 5].

Schedule 40 black iron pipe has a wall thickness of approximately 2.5 to 3.5 mm — 10 to 15 times the wall thickness of CSST. The ICLP 2012 paper [2] demonstrated through both field-incident analysis and controlled laboratory testing that lightning routinely creates holes in CSST under conditions representing partial lightning currents, not only direct strikes. The perforation hazard therefore extends to induced currents from nearby strikes, side flashes, and ground current propagation within the structure.

2.2. Jacket Dielectric Properties and the Breakdown Threshold

The PE jacket of standard yellow CSST serves as the primary dielectric barrier between the external electromagnetic environment and the stainless steel gas tube wall. The Gas Technology Institute (GTI) lightning hole study [5, 25] characterized the dielectric breakdown properties of the CSST jacket using lightning-type impulse waveforms (1.2/50 µs rise/fall time), consistent with the IEC 60060-1 standard [48] for high-voltage testing.

Table 1
CSST Arc Perforation Likelihood as a Function of Action Integral. Derived from GTI laboratory testing [5, 24, 25] and ICLP 2012 field and laboratory data [2]. Approximate I_{peak} values for 8/20 µs waveform. Complete derivations and step-by-step calculations are provided in [50].

Action Integral $\int I^2 dt$ (A²·s)	I_{peak} Approx. (8/20 μs)	Perforation Outcome
$< 10^2$ (<100)	<2 kA	No perforation — safe region
10^2–10^3 (100–1000)	2–8 kA	Transition zone; occasional melt-through
$> 10^3$ (>1000)	8–15 kA	Perforation likely — melt and ejection
$> 10^4$ (>10,000)	≥30 kA	Perforation almost certain
10^5–10^6	~30 kA median	Exceeds threshold by 10^2–$10^3\times$

The GTI investigation established jacket dielectric breakdown at applied impulse voltages of approximately 25 to 35 kV peak — substantially lower than the DC or power-frequency breakdown voltage of the same jacket material. Under the steep-fronted, high-amplitude voltage transients characteristic of lightning coupling, the jacket breaks down at significantly lower voltages than laboratory-frequency testing might suggest. Once the CSST jacket dielectric breakdown occurs, the resulting arc channels to the stainless steel wall, depositing sufficient energy for perforation according to the current and waveform parameters.

2.3. The Action Integral: A Quantitative Perforation Failure Model

The governing physical parameter for arc-induced burn-through in metallic conductors is not peak current alone but the action integral — the integral of the square of current over the duration of the discharge. This parameter, with units of A^2 s, directly quantifies the specific energy deposited in the arc attachment zone:

$$\text{Action Integral} = \int_0^{\tau} I^2(t)\, dt \quad [\text{A}^2\,\text{s}] \tag{1}$$

The physical basis is that Joule heating in the arc attachment region scales as I^2R, so the total thermal input to the melting zone is proportional to $\int I^2\, dt$. For standard lightning waveform approximations:

$$\int I^2\, dt \approx k \cdot I_{\text{peak}}^2 \cdot t_{\text{half}} \tag{2}$$

where $k \approx 0.5$ for the 8/20 µs waveform and $k \approx 0.6$–0.7 for the 10/350 µs waveform, and t_{half} is the waveform half-value time (derivation of both k values from the double exponential waveform model is provided in [50]).

Drawing on GTI experimental data [5, 24, 25] and the ICLP 2012 results [2], Table 1 establishes the empirical failure boundary for standard CSST at 0.25 mm wall thickness.

Note: The failure thresholds represent approximate ranges derived from limited experimental datasets. Variability in material properties, arc attachment conditions, and waveform characteristics may influence the precise onset of perforation. The action integral framework should be interpreted as an engineering approximation for comparative analysis rather than a deterministic predictor of failure.

The practical perforation criterion can therefore be stated as:

$$\text{Perforation likely if:} \quad \int I^2\,dt \gtrsim 10^3 \text{ A}^2\text{ s} \tag{3}$$

with failure becoming almost certain at $\int I^2\,dt > 10^4$ A^2 s. A typical negative first return stroke has a median peak current of 30 kA [7, 28]. For a 10/350 µs waveform, this corresponds to an action integral of approximately 10^5 to 10^6 A^2 s — exceeding the CSST perforation threshold by two to three orders of magnitude. The ICLP 2012 analysis [2] confirmed perforation in laboratory and field conditions representing partial lightning current at 5 to 10 kA, placing these events squarely in the transition-to-failure region of Table 1.

The SEFTIM/FPRF Phase 1 investigation [27] explicitly identified this induced-surge scenario as a credible damage mechanism, noting that CSST has increasingly become one of the few remaining metallic current paths in modern American homes — as plastic water pipe, wireless networking, and non-metallic conduit have displaced traditional metallic infrastructure — concentrating induced lightning current onto the CSST run. The forensic correlation between the physical perforation mechanism and the observed fire patterns is further documented in [8, 26].

3. The Cloud-to-Ground Circuit and the Ungrounded Roof Electrode Array

3.1. Cloud-to-Ground Lightning: Circuit Topology

A lightning discharge is an electrostatic discharge event driven by charge separation between the thundercloud base — typically negatively charged — and the earth's surface. During thunderstorm approach, the electrostatic field induces charge redistribution on all conductive objects at or near the surface. Grounded conductors dissipate induced charge to earth; electrically isolated metallic objects accumulate charge toward the local cloud-induced ambient potential. This is an unconditional consequence of the Maxwell equations for any conductor in an external electric field [21]. The dart-leader phase propagates from the cloud base toward earth, establishing a low-impedance plasma channel. The return stroke follows within microseconds, driving a current pulse of typically 10 to 100 kA peak through the earth connection [7, 28].

3.2. The Ungrounded Roof Electrode Array

A residential roof assembly contains thousands of electrically isolated metallic elements: roofing nails, deck screws, ridge cap fasteners, flashing hardware, HVAC mounting brackets, and conduit clamps. These are embedded in wood framing and dielectric insulating materials, separated from the building's grounding electrode system by continuous non-conductive layers. They cannot, as a practical engineering matter, be individually bonded or grounded.

This configuration has direct electromagnetic consequences under thunderstorm conditions. Electrically isolated conductors have no dissipation path and therefore accumulate surface charge toward the local cloud-referenced ambient potential through electrostatic induction. This is an unconditional consequence of the Maxwell equations, independent of the conductor's geometry, mass, or orientation [9, 21]. The process requires no visible discharge manifestation to be physically effective.

The experimental literature on floating electrode systems in high-voltage and thunderstorm-magnitude fields confirms that these elements are not passive charge accumulators. Under the intensifying field of an approaching lightning leader, isolated sharp-tipped conductors generate corona discharge, reduce the aggregate breakdown voltage of the surrounding air gap geometry, and interact collectively through field coupling — the thousands of geometrically varied fasteners across a roof deck producing distributed discharge initiation across a continuous range of local breakdown thresholds rather than a discrete simultaneous event [35, 36, 37, 38, 39, 40, 47]. The spark-to-impulse field conversion mechanism documented in the complex gap literature [35] establishes that this activity intensifies non-linearly under the fast-fronted field rise characteristic of leader approach.

The roof fastener array constitutes a distributed cloud-potential electrode system suspended above CSST runs in the attic below. The potential difference between this floating array and the CSST — placed at ground or GPR-elevated ground potential through its bonding connection — is the arc-driving voltage for jacket breakdown and wall perforation. No published study has specifically characterised this arc transfer pathway in the context of residential CSST installations. This paper identifies it as the principal proposed arc source and a substantive gap in the existing research literature requiring experimental investigation. This pathway is entirely outside the bonding system: no connection between CSST and any grounded conductor in the building reduces the potential difference between the cloud-potential roof fastener array and the gas tube below.

3.3. Experimental Visual Evidence: Ground Current Energization of Structural Conductors

The claim that bonded structural conductors are actively energized during a lightning event — rather than remaining at a stable ground reference potential — is supported by a convergent body of experimental observational evidence.

The most direct visual confirmation is provided by Saba et al. [6], whose high-speed optical study captured photographic evidence of upward-propagating streamers growing from a grounded structural steel building element toward a

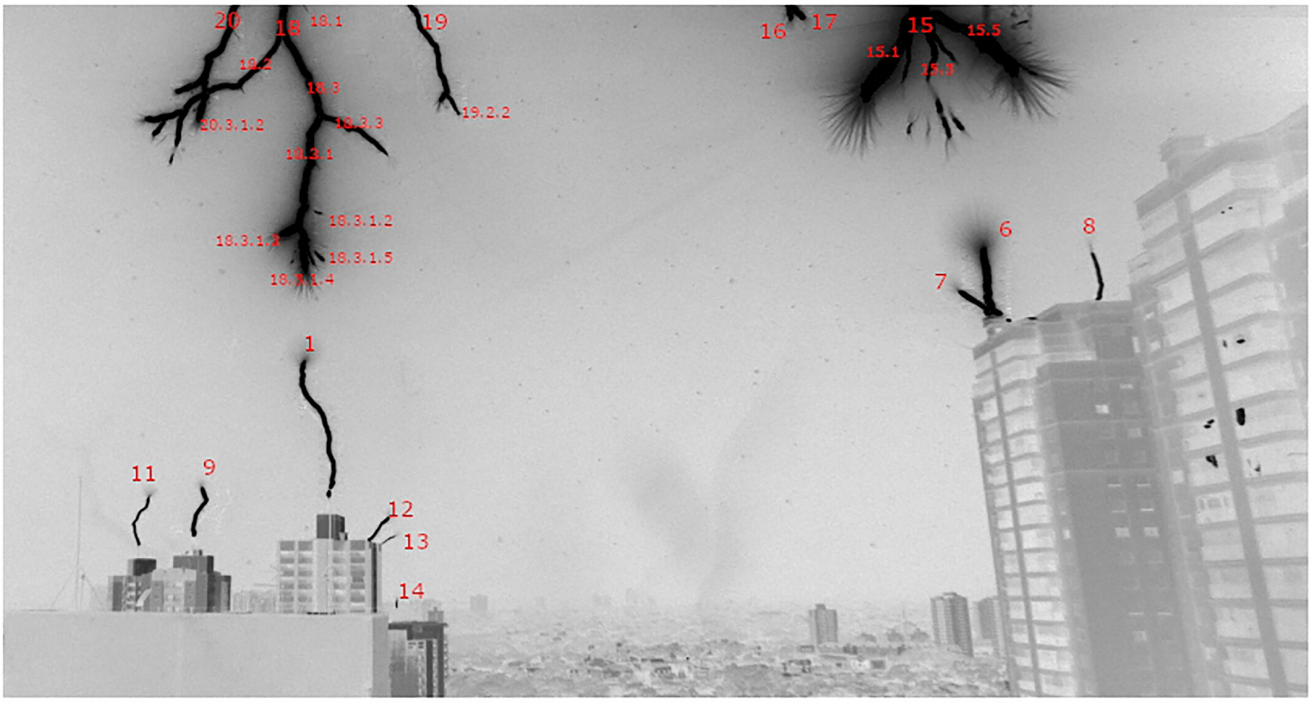

Figure 1: Reproduced without modification from Saba et al. (2022), Figure 2 [6]. High-speed optical image showing upward-propagating positive streamers from a grounded structural steel building element toward the downward-propagating negative leader, providing direct visual confirmation of Ground Potential Rise energisation of bonded structural conductors during the lightning attachment process. © 2022 Saba et al., *Geophysical Research Letters*, 49(24), e2022GL101482. Reproduced under CC BY-NC-ND 4.0.

downward-propagating leader. Grounded metallic structural conductors do not remain at zero potential during a lightning event — they develop streamers, the observable signature of a conductor driven to an elevated transient potential by the local field conditions.

Figure 1 provides direct photographic confirmation of this energization: GPR recorded on film. Figure 2 shows the physical result at the chimney attachment point of the same event: concrete displaced, structural steel exposed, following a return stroke of −29.6 kA — median by the natural lightning distribution [7, 28]. The same class of return stroke energisation is communicated to bonded CSST through its mandatory connections. Unlike the chimney's reinforced concrete, which can sustain and visibly document that energy deposition, the 0.25 mm stainless steel wall of CSST perforates silently at a fraction of that energy — and releases the gas behind it.

4. Ground Potential Rise and the Physical Failure of the Bonding Mandate

4.1. Ground Potential Rise: Physical Basis

Ground Potential Rise (GPR) refers to the transient elevation of potential at a grounded structure's grounding electrode above true remote earth potential during a lightning discharge. For a grounding electrode with resistance R_g and inductance L_g, the peak GPR during a return stroke with peak current I_p and peak rate of change dI/dt is:

$$V_{\mathrm{GPR}}(t) = R_g I(t) + L_g \frac{dI}{dt} \tag{4}$$

For a typical negative first return stroke with $I_p = 30$ kA and $dI/dt \approx 10$ to 100 kA/μs [7, 28] and representative residential grounding parameters of $R_g = 5\ \Omega$ and $L_g = 5$ μH, the inductive term alone contributes 50 to 500 kV to the peak GPR — well above the jacket dielectric breakdown threshold established in Section 2.2 [5]. Vieira et al. [46] conducted peer-reviewed electromagnetic simulations and measurements of GPR in interconnected grounding systems, demonstrating that GPR propagates through all conductors bonded to the grounding system and that the presence of aerial metallic elements significantly increases the GPR peak for fast-fronted currents due to their inductive contribution.

The ICC bonding mandate requires CSST to be electrically connected to the grounding electrode system through water piping, structural steel, or electrical raceways. When GPR is elevated to V_{GPR} during a lightning event, this potential is communicated to the CSST through its bonding connection. If V_{GPR} exceeds the impulse breakdown voltage of the CSST PE jacket (Section 2.2 [5]), arc perforation follows. The field measurement evidence established in Section 3.3 [45] confirms that GPR transmission through interconnected grounding conductors is a directly observed physical phenomenon in instrumented real-world installations. The bonding mandate has instead connected CSST

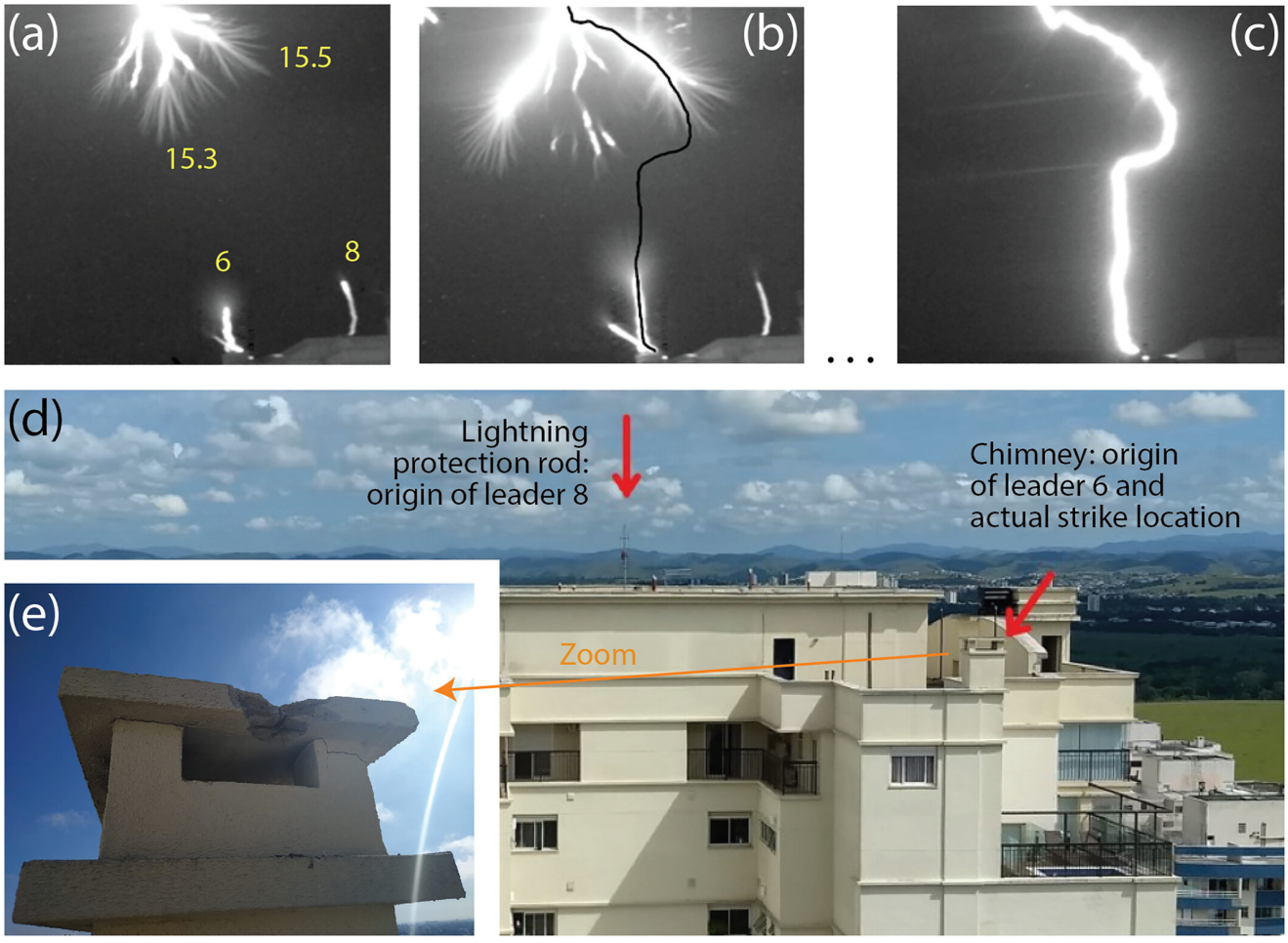

Figure 2: Reproduced without modification from Saba et al. (2022), Figure 5e [6]. Physical destruction of the chimney attachment point following a −29.6 kA return stroke, with concrete displaced and structural steel exposed at the arc attachment location. © 2022 Saba et al., *Geophysical Research Letters*, 49(24), e2022GL101482. Reproduced under CC BY-NC-ND 4.0.

to the conductor network that carries the highest transient potential in the building during the event.

4.2. The Bonding Mandate's Physical Rationale and Its Refutation

The ICC CodeNotes for IFGC §310.2 state that the purpose of CSST bonding is to minimise the potential difference between CSST and other metallic systems in the building, thereby reducing the risk of arcing between them [11]. This rationale is physically valid for the inter-conductor arcing scenario. However, the principal proposed arc scenario is not inter-conductor arcing within the building — it is arcing between the ungrounded roof fastener array at cloud potential and the CSST below at ground or GPR-elevated potential. Furthermore, the upward streamer observations of Saba et al. [6], Tran and Rakov [41], and Cummins et al. [42] — whose physical basis in the quantitative relationship between external field strength and streamer zone charge is established by Cooray et al. [43] — confirm that the grounded structural conductors to which CSST is bonded are not maintained at a stable ground reference during the event. Schumann, Saba et al. [44] further established that the continuing current phase following a nearby return stroke is the most effective trigger for upward leader initiation from grounded structures, confirming that the window of GPR-induced transient voltage exposure on a bonded CSST installation extends across the full duration of nearby lightning activity.

The simulation study by Haslam, Galler, and Eagar [13] found that for the scenario where lightning enters through an outdoor light fixture or chimney, the presence of a grounding wire increases the charge delivered through the arc from 0.13 C to 2.22 C — a 17-fold increase attributable directly to the bonding connection. For lightning strikes with peak current at or above the median of the natural distribution, there was no simulation scenario in which grounding succeeded in preventing perforation [13]. The SEFTIM/FPRF Phase 1 investigation [27] independently concluded that bonding is probably not the only solution and that a global equipotential solution is necessary to achieve complete protection. Achieving true equipotentiality across all metallic elements of a building during a lightning transient — the architecture of an aircraft-grade Faraday cage enclosure per RTCA DO-160G [18] — is physically unachievable for an existing

residential structure. The logical corollary is that the only remaining engineering path consistent with the physics is to provide local electromagnetic shielding of the vulnerable conductor itself, developed in Section 6.

4.3. The Three Arc Failure Modes of Bonded CSST

A complete analysis of bonded CSST identifies three distinct arc failure modes that bonding either fails to address or actively exacerbates:

Mode 1 — Roof Electrode Array Arc: The principal proposed arc pathway failure mode. The ungrounded roof fastener array at cloud potential arcs to the CSST. Bonding does not reduce the cloud-to-ground potential difference. GPR elevation of the bonded CSST increases the driving potential for this arc. Bonding provides zero protective benefit against Mode 1 and may increase Mode 1 risk [3, 13].

Mode 2 — GPR-Driven Jacket Breakdown: If CSST is bonded to a conductor experiencing GPR and the GPR voltage reaches or exceeds the impulse breakdown voltage of the CSST jacket (Section 2.2 [5]), the jacket fails and arc perforation occurs. The peer-reviewed GPR measurement evidence [46] and field transient propagation observations [45] confirm that these voltage levels are physically realised in interconnected residential-scale grounding systems during energetic return strokes. This failure mode exists only in bonded installations.

Mode 3 — Bonding-Enabled AC Fault Current Arcing: Unbonded CSST has no complete circuit to ground when a live AC conductor contacts it, limiting fault current naturally. The bonding mandate removes this protection by establishing a low-impedance return path to ground at every point along the run, converting an incidental exposure into a sustained arcing hazard at the stainless steel wall. While an unbonded installation retains some residual AC fault current exposure through capacitive coupling or arc paths to adjacent bonded conductors, the bonding mandate substantially exacerbates this risk by providing a direct, low-impedance return path. Retrofit shielding addresses Mode 3 through two sequential defences: physical exclusion of live conductors across the full protected length as the primary layer, and conductive fault current diversion to ground as the secondary — with residual exposure confined to the geometrically limited transition zones at manifold, iron pipe junction, and appliance terminus.

This analysis is consistent with the documented pattern of CSST fires in fully bonded and grounded installations, including the death of Brennen Chase Teel in Lubbock, Texas in August 2012 in a home where CSST was installed and bonded per manufacturer specifications and applicable building codes. Despite the bonding mandate being in place for nearly a decade at the time of reporting, investigative journalism by Scott Friedman of NBC DFW documented continued CSST fires in bonded installations, with an independent engineer Mitch Guthrie and member of the NFPA Lightning Protection Committee stating that grounding and bonding 'won't prevent all incidents' [49].

5. The Coaxial Cable Analogy: The Architecture That Was Not Applied

5.1. Structural Equivalence of CSST and Coaxial Cable

A coaxial cable consists of two concentric conductors separated by a dielectric layer: an inner signal-carrying conductor and an outer conductive shield that functions as a Faraday cage, distributing all induced charge on its exterior surface and leaving the interior field-free. CSST is structurally equivalent to a coaxial cable in which the gas-carrying stainless steel tube occupies the role of the inner conductor. Both are metallic tubular conductors enclosed within a dielectric jacket, both transport a payload that must not be exposed to external electromagnetic energy, and both are governed by the same Maxwell equations for induced current and arcing. The critical difference is that the telecommunications coaxial cable has an outer conductive shield and CSST does not. National Electrical Code NFPA 70 Article 800 mandates electromagnetic shielding for residential telecommunications conductors [17] precisely because the industry recognised that an unshielded inner conductor would collect lightning-induced transients and fail. The same physics applies, with greater urgency, to the gas tube carrying explosive natural gas through the same wall spaces.

5.2. The Fundamental Error of the Bonding Mandate in Coaxial Terms

The coaxial cable analogy makes the physical error of the ICC bonding mandate immediately apparent. The inner conductor of a coaxial cable is not bonded to the outer shield — it is isolated from it by the dielectric layer. The protective mechanism is electromagnetic isolation of the inner conductor from external fields by the outer shield, not connection to it. The bonding mandate requires the functional equivalent of connecting the inner signal conductor of a coaxial cable to its outer shield and to every other grounded metallic conductor in the building — the precise configuration that defeats the protection.

A typical five-appliance gas installation carries 150 to 300 feet of CSST through attic and wall spaces; a comparable coaxial cable installation totals 50 to 100 feet. There is more CSST than coaxial cable in the same building, carrying a payload with far more severe consequences of electrical failure — explosive gas release rather than signal interruption — yet the less critical conductor is mandated to be electromagnetically shielded while the more critical one is connected to the grounding system in precisely the configuration that defeats that protection. NEC Article 800 requires shielding for coaxial cable to protect a data connection from transients. CSST carries explosive natural gas. With an unshielded CSST run, the result is not a dropped connection — it is a gas-fed structural fire.

6. Retrofit Electromagnetic Shielding: The Faraday Cage Solution

6.1. Gauss's Law and the Field-Free Interior

The physical principle governing electromagnetic shielding effectiveness is Gauss's Law, one of the four Maxwell equations [21, 22]. For a closed conductive surface S enclosing a volume V, Gauss's Law states:

$$\oint_S \vec{E} \cdot d\vec{A} = \frac{Q_{\text{enc}}}{\epsilon_0} \tag{5}$$

For a closed conductive shell in electrostatic equilibrium, the free charges redistribute on the outer surface under any external field, producing zero field inside the conductor and zero field within the enclosed volume. This result is the mathematical basis of the Faraday cage, first demonstrated experimentally by Michael Faraday in 1836 [23]. It is exact and unconditional: for any closed conductive shell of any geometry, the enclosed interior is completely free of the external electric field, regardless of the magnitude or spatial distribution of external charges or fields.

Two complementary shielding mechanisms operate sequentially across a lightning event. During the quasi-static pre-stroke phase, *electrostatic shielding* governed by Gauss's Law prevents arc initiation from the roof fastener array: the closed conductive enclosure redistributes surface charge to maintain zero internal field regardless of the intensifying external potential. This mechanism is frequency-independent and requires only geometric closure — it does not depend on shield thickness or skin depth. During the return stroke itself, *dynamic electromagnetic shielding* governed by Faraday's law of induction attenuates the rapidly time-varying magnetic field through eddy current opposition in the shield conductor, with effectiveness scaling with frequency as quantified below. The two mechanisms are sequential: the electrostatic mechanism prevents arc initiation during the pre-stroke build-up phase, and the dynamic mechanism attenuates the residual electromagnetic transient during the return stroke. A continuously closed retrofit shield engages both across the full duration of the event.

For dynamic electromagnetic fields, the shielding effectiveness SE of a conductive enclosure is quantified in decibels as:

$$\text{SE} = 20 \log_{10}\left(\frac{|E_{\text{incident}}|}{|E_{\text{transmitted}}|}\right) \text{ dB} \tag{6}$$

For a continuous conductive enclosure with no apertures, SE is limited only by the skin depth δ of the shield material [21]:

$$\delta = \sqrt{\frac{2}{\omega\mu\sigma}} \tag{7}$$

where ω is the angular frequency, μ is the magnetic permeability, and σ is the electrical conductivity of the shield material.

For stainless steel ($\sigma \approx 1.4 \times 10^6$ S/m, $\mu \approx \mu_0$) at 100 kHz — representative of the dominant low-frequency energy content of a lightning return stroke — the skin depth evaluates to approximately 1.35 mm. The CSST wall itself (0.25 mm) represents only approximately 0.19 skin depths; a retrofit shield of 0.5 to 1.0 mm thickness provides approximately 0.37 to 0.74 skin depths at this frequency. At 1 MHz, $\delta \approx 0.43$ mm and a 1.0 mm shield provides approximately 2.3 skin depths (SE $\approx$ 20 dB from skin-effect alone); at 9 MHz, $\delta \approx 0.14$ mm and a 1.0 mm shield provides approximately 7 skin depths (SE $\approx$ 60 dB). For the low-frequency and quasi-static components that dominate the lightning action integral, the primary shielding mechanism is the electrostatic boundary condition of the closed Faraday cage enclosure, guaranteed by Gauss's Law to produce a field-free interior regardless of skin depth. The two mechanisms are therefore complementary.

The critical design requirement is shield continuity: the Faraday cage must be closed from manifold to appliance terminus with no apertures. A break in shield continuity — even a small gap — allows penetration of external electromagnetic energy and eliminates the Gauss's Law guarantee.

6.2. Retrofit Installation Design

The retrofit shielding solution must satisfy two engineering constraints simultaneously: (1) it must form a continuous Faraday cage from the gas manifold to every appliance connection; and (2) it must be installable over existing CSST without disturbing the gas system. These constraints are satisfied by a split-sleeve side-entry conductive conduit design: a conductive conduit manufactured with a longitudinal slit allowing it to be opened radially, positioned around the existing CSST run, and closed to form a continuous conductive enclosure.

The retrofit installation does not require gas permits, does not disturb any gas fitting or connection, and can be performed with the gas system in service. The installation labour for a typical five-appliance residential system is estimated at 3 to 6 hours for a certified installer. For CSST sections fully encased within finished drywall or otherwise inaccessible, the affected run must be re-routed or replaced with a new shielded-accessible installation. These costs remain marginal when evaluated against the alternative: fire and lightning claims represent the costliest category of homeowners losses, with an average claim of $88,170 for the period 2019–2023 [29].

6.3. Protection Against AC Fault Currents

The retrofit shield's two-layer protection against 60 Hz AC fault current arcing — physical exclusion as the primary defence across the full protected run, and conductive fault current diversion as the secondary defence at any point of jacket breach — is developed in the context of Mode 3 in Section 4.3. The outer shield must be bonded to the grounding system rather than the inner CSST gas tube, restoring the correct coaxial cable architecture described in Section 5.

6.4. Verification and Inspection

The effectiveness of an installed retrofit shield is directly verifiable by measurement. Shield continuity — the critical parameter ensuring Faraday cage integrity — can be verified using a standard continuity tester or low-resistance ohmmeter. A well-installed, continuous shield will present near-zero resistance from one terminus to the other. This verification step, performed at installation and at periodic inspection intervals, provides documented confirmation of shield integrity that is not available for any other CSST fire protection measure. The bonding mandate, by contrast, does not verify or address the principal proposed arc source — the ungrounded roof electrode array.

7. Arc-Resistant CSST Products: Incomplete Faraday Cage Implementations

7.1. Product Architectures

In response to documented CSST lightning fires and associated litigation, CSST manufacturers developed arc-resistant product lines. The principal commercial products — CounterStrike (OmegaFlex), WARDFlex Max (Ward Manufacturing), and FlashShield (Gastite/Titeflex) — employ different design approaches that can be evaluated against the Faraday cage physics established in Section 6.

7.2. Conductive Polymer Products: CounterStrike and WARDFlex Max

CounterStrike and WARDFlex Max employ a conductive carbon-black-filled polymer jacket in place of the standard insulative polyethylene jacket of yellow CSST. The design intent is to provide a conductive outer surface that distributes arc energy. However, the conductive polymer implementation introduces a critical failure mode not present in yellow CSST: the conductive jacket creates a low-resistance current path from any contacting 60 Hz AC source directly to the stainless steel tube wall.

This failure mode was documented in independent testing commissioned by the National Association of State Fire Marshals (NASFM) and performed by Integrity Forensics and Engineering, LLC [16]. Under standardised 120-volt AC fault conditions, CounterStrike produced stainless steel wall perforations and gas-fed fires in 4 of 5 test samples. WARDFlex Max produced perforations and fires in all 5 of 5 test samples. Standard yellow CSST produced zero perforations in 5 of 5 tests [16]. From the perspective of Faraday cage physics, the conductive polymer products are doubly deficient: conductive polymer has electrical conductivity substantially lower than metallic conductors, providing lower shielding effectiveness at lightning-relevant frequencies; and the continuous resistive current path does not prevent arc initiation once the threshold for air gap breakdown is exceeded.

7.3. Metallic Mesh Products: FlashShield

FlashShield employs a multi-layer jacket incorporating a conductive aluminum mesh between dielectric layers. This architecture is a closer approach to the correct Faraday cage design. FlashShield's manufacturer markets the product with reference to aerospace lightning protection standards [15]. However, two structural vulnerabilities compromise this implementation.

Shield Continuity at Fittings: FlashShield's electromagnetic shield terminates at every gas fitting junction. Any use of a standard CSST fitting creates a gap in the Faraday cage with no visual indication of the breach from outside the jacket. Any subsequent service work involving a plumber who has no knowledge of the FlashShield XR3 fitting requirement will result in a standard fitting being installed from stock, breaking the Faraday cage at that junction while the homeowner continues to believe the system is protected. This is a systematic and latent failure mode that compounds over the service life of the installation with every subsequent gas system modification, and it is invisible without disassembly and inspection of every fitting in the run.

Galvanic Corrosion at Dissimilar-Metal Interfaces: The XR3 fittings create junctions between the aluminum mesh of the FlashShield jacket and brass CSST fitting bodies. Aluminum is substantially more anodic than brass in the electrochemical galvanic series, with a standard potential difference of approximately 0.6 V in aqueous environments [30] — a dissimilar-metal pairing classified as high-risk under MIL-STD-889D [31]. In the attic and crawlspace environments typical of CSST installations, seasonal condensation cycling provides the aqueous electrolyte necessary to sustain this galvanic couple, progressively degrading the aluminum mesh at each fitting junction.

The galvanic behaviour of aluminum-to-dissimilar-metal interfaces in shielded cable and connector systems is well characterised in the peer-reviewed literature [32, 33, 34]. Most directly analogous is the progressive degradation of electromagnetic shielding effectiveness at the aluminum-braid-to-connector interface of coaxial cable F-connectors through galvanic attack, identified as the primary failure mode of that interface in a CableLabs-funded electrochemical study [34]. The aluminum mesh to brass fitting junction of FlashShield is electrochemically equivalent to the F-connector interface characterised in [34]. No peer-reviewed or publicly available corrosion characterisation of the FlashShield aluminum mesh to XR3 brass fitting interface under residential installation conditions appears in the open literature. The only available physical characterisation is the expert testimony of Rasty and Dickens [14], conducted on behalf of a commercial competitor and presented in a municipal council proceeding rather than a peer-reviewed venue.

8. Discussion: Implications for Building Codes, Engineering Practice, and Fire Safety

8.1. Required Code Revision

The analysis developed in this paper leads to two principal code revision recommendations: (1) replacement of

the current CSST bonding mandate (ICC IFGC §310.2; IRC G2411.2) with a requirement for continuous retrofit electromagnetic shielding; and (2) adoption of an electromagnetic shielding performance standard for CSST analogous to the shielding requirements for residential telecommunications conductors under NEC Article 800. The physical basis for both recommendations is established in Sections 4.1 through 4.3, which demonstrate that the bonding mandate fails to address any of the three identified arc failure modes and actively exacerbates two of them.

8.2. Precedents for Mandatory Electromagnetic Shielding in Comparable Applications

The requirement for electromagnetic shielding of vulnerable conductors in environments subject to lightning transients has been codified across multiple regulatory frameworks:

- **NEC Article 800:** Mandates shielded cable for all residential telecommunications conductors — the direct analogue of CSST shielding, applied to the data cable in the same wall spaces as the gas tube [17].
- **RTCA DO-160G:** Lightning indirect effects shielding requirements for aircraft systems, including fuel system components — the direct aerospace precedent for shielding fuel-carrying conductors [18].
- **IEC 61511:** Mandates shielded instrumentation wiring in all facilities handling flammable gases [20].
- **IEC 61000-4-5:** Surge immunity requirements for equipment connected to building infrastructure subject to lightning transients [19].

8.3. Limitations and Future Work

The action integral failure model presented in Section 2.3 represents an engineering approximation derived from the available GTI and ICLP experimental data; the complete source data, waveform derivations, and uncertainty bounds underpinning that model are documented in [50]. A complete probabilistic failure model would require systematic testing across the full distribution of lightning waveform parameters — including both 8/20 µs and 10/350 µs standard waveforms — with statistical characterisation of the failure boundary as a function of both I_{peak} and waveform duration. Future work should also address the electromagnetic modelling of the roof electrode array geometry and its coupling to specific CSST routing configurations, informed by the corona physics of Roman et al. [9] and Azadifar et al. [10].

9. Conclusion

This paper has developed a comprehensive physical framework for the CSST lightning fire hazard and demonstrated that retrofit electromagnetic shielding is the only engineering solution consistent with the physics of the hazard. The key findings are as follows:

- CSST perforates. Its 0.15 to 0.25 mm stainless steel wall fails at action integral thresholds that median lightning exceeds by two to three orders of magnitude, and laboratory testing confirms perforation under partial lightning currents representing only a fraction of a typical strike [2, 3, 5]. The thinness that makes CSST flexible makes it indefensible against lightning energy by any bonding or grounding measure that leaves the wall thickness and jacket breakdown voltage unchanged.
- Lightning discharge transfers energy between the charged cloud base and the earth regardless of whether attachment is initiated from above or below. The ungrounded metallic roof fastener array — thousands of electrically isolated nails, screws, and hardware elements suspended above CSST runs at attic level — sits across this potential difference during the entire pre-stroke build-up phase, accumulating charge toward cloud potential through electrostatic induction [9, 35, 39]. No published study has characterised the arc transfer from this distributed floating array to residential CSST below it. This paper identifies that pathway as the principal proposed arc source and a specific gap in the existing research literature warranting experimental investigation.
- Three arc failure modes have been identified. Mode 1 is arc initiation from the roof fastener array — the proposed principal pathway, entirely outside the bonding system. Mode 2 is GPR-driven jacket breakdown: the ICC bonding mandate communicates return stroke ground potential rise to the gas tube through its required connections to structural steel, water piping, and electrical raceways, elevating the CSST to the highest transient potential in the building during the event [6, 13, 46]. Mode 3 is bonding-enabled AC fault current arcing: the bonding connection converts an incidental exposure into a reliably complete fault circuit at every point along the CSST run. The bonding mandate addresses none of these modes — it exacerbates Mode 2, substantially increases Mode 3 risk, and is physically incapable of reducing the cloud-to-ground potential difference that drives Mode 1 [3, 13, 27].
- Arc-resistant CSST products are structurally flawed implementations of the Faraday cage shielding principle. Conductive polymer products introduce the Mode 3 failure that standard yellow CSST does not exhibit, producing perforations and fires at ordinary 120 V household current [16]. FlashShield's metallic mesh architecture approaches the correct design but is compromised by fitting-dependent continuity gaps that are invisible without disassembly, and by galvanic corrosion at the aluminium-to-brass interface for which no independent characterisation exists [30, 31, 34]. No current product addresses all three failure modes simultaneously, and none is field-verifiable.

- Retrofit electromagnetic shielding — a continuous conductive enclosure applied from manifold to appliance terminus without gas system disturbance — is the only measure that resolves all three failure modes. It intercepts Mode 1 before the arc reaches the wall. It isolates the gas tube from the GPR-energised grounding system, eliminating Mode 2. It physically excludes live conductors across the full protected run and diverts any breach current to ground, addressing Mode 3. Its shield continuity is directly measurable by standard instrumentation — the only quantitative field-verifiable protection parameter available for any CSST installation. Retrofit shielding applied over any CSST type — including arc-resistant CSST — corrects the deficiencies of that product's incomplete Faraday cage implementation.

These findings have direct implications for the more than six million American homes containing an estimated one billion feet of unshielded CSST [1]. The ICC bonding mandate, in place for nearly two decades, has governed installation practice while failing to address — and in two of three modes actively worsening — the hazard it was designed to mitigate. Building codes should require continuous retrofit electromagnetic shielding for all CSST types and rescind the bonding mandate. Future research should focus on experimental characterisation of the roof fastener array arc pathway to close the gap identified here, and on probabilistic perforation modelling across the full lightning current distribution to provide the actuarial foundation for regulatory prioritisation.

Conflict of Interest Statement

The author is the founder and CEO of PyroThor LLC (https://pyrothor.com), a company that manufactures and markets a retrofit electromagnetic shielding jacket system for CSST. The solutions described in this paper represent a class of engineering approaches to the CSST lightning hazard; the author's commercial product is one implementation of the principles discussed herein.

CRediT authorship contribution statement

Ramanathan Karthikeyan: Conceptualization, Methodology, Writing – Original draft preparation.

References

[1] U.S. Fire Administration (FEMA). National Fire Incident Reporting System (NFIRS): CSST Coding Help. Available from: https://www.usfa.fema.gov/nfirs/coding-help/csst/ [accessed April 2026].

[2] Rousseau A, Guthrie M. Direct lightning withstand of corrugated stainless steel tubing for gas. In: Proc. Int. Conf. Lightning Protection (ICLP); 2012; Vienna, Austria. Available from: https://seftim.com/wp-content/uploads/2015/11/ICLP_2012_Direct-Lightning-Withstand-of-Corrugated-Stainless.pdf [accessed April 2026].

[3] Haslam B, Eagar TW. Variation in lightning simulations to assess grounding safety of corrugated stainless steel tubing (CSST). Fire Technol. 2020;56:425–444. https://doi.org/10.1007/s10694-019-00885-x

[4] Goodson M, Hergenrether M. Lightning induced CSST fires. In: Fire and Materials 2005 Conference Proceedings; 2005 Jan 31–Feb 1; San Francisco, CA. London: Interscience Communications; 2005. Available from: https://lightning.org/wp-content/uploads/2014/12/CSST_-_Interscience_2005_Report.pdf [accessed April 2026].

[5] Hammerschmidt A, Ziolkowski CJ. Validation of installation methods for CSST gas piping to mitigate indirect lightning related damage: final report. GTI Project No. 21323. Des Plaines (IL): Gas Technology Institute; 2013. Available from: https://brennenteelfoundation.org/wp-content/uploads/SEFTIS-Report-GTI-CSST-Final-Report-Amended-9-5-13-1.pdf [accessed April 2026].

[6] Saba MMF, da Silva DRR, Pantuso JG, da Silva CL. Close view of the lightning attachment process unveils the streamer zone fine structure. Geophys Res Lett. 2022;49(24):e2022GL101482. https://doi.org/10.1029/2022GL101482

[7] Berger K, Anderson RB, Kroninger H. Parameters of lightning flashes. Electra. 1975;(41):23–37.

[8] Goodson M, Hergenrether M. Investigating the causal link between lightning strikes, CSST and fire. Fire & Arson Investig. 2005 Oct. Available from: https://goodsonengineering.com/wp-content/uploads/2017/10/Investigating-the-Casual-Link-Between-Lightning-Strikes-CSST-Fire.pdf [accessed April 2026].

[9] Roman F, Cooray V, Scuka V. Corona from floating electrodes. J Electrostat. 1996;37(1–2):67–78. https://doi.org/10.1016/0304-3886(96)00005-8

[10] Azadifar M, Li D, Rachidi F, Rubinstein M, Diendorfer G, Pichler H, et al. Observations of corona point discharges from grounded rods under thunderstorms. Atmos Res. 2020;243:105238. https://doi.org/10.1016/j.atmosres.2020.105238

[11] International Code Council (ICC). CodeNotes: bonding of corrugated stainless steel tubing (CSST) gas piping systems. Building Safety Journal. 2020 Jul 6. Available from: https://www.iccsafe.org/building-safety-journal/bsj-technical/codenotes-bonding-of-corrugated-stainless-steel-tubing-gas-piping-systems/ [accessed April 2026].

[12] U.S. Fire Administration (USFA). ATF investigation report on lessons learned from 2 line-of-duty deaths [blog post]. U.S. Department of Homeland Security; 2023 Aug 10. Available from: https://www.usfa.fema.gov/blog/atf-investigation-report-on-lessons-learned-from-2-lodd/ [accessed April 2026].

[13] Haslam B, Galler D, Eagar TW. Fire safety of grounded corrugating stainless steel tubing in a structure energized by lightning. Fire Technol. 2016;52(2):581–606. https://doi.org/10.1007/s10694-015-0557-z

[14] Rasty J, Dickens J. Expert testimony of Jahan Rasty, Ph.D., P.E. and James Dickens, Ph.D., P.E. on behalf of OmegaFlex, Inc. City of Lubbock, Texas Regular City Council Meeting; 2016 May 12. Available from: https://brennenteelfoundation.org/wp-content/uploads/2018/01/Lubbock-City-Council-Testimony-Excerpts3.pdf [accessed April 2026].

[15] Gastite. FlashShield CSST with XR3 fitting (SS-FlashXR3). Titeflex Corporation; 2018. Available from: https://www.gastite.com/downloads/pdfs/ss-flashxr3.pdf [accessed April 2026].

[16] Tracy TG, Colwell K, Spruiell JP. 120 volt household current testing on corrugated stainless-steel tubing types and schedule 40 black iron gas piping. Integrity Forensics and Engineering, LLC. Prepared for: National Association of State Fire Marshals; 2018 Feb 22. Available from: https://brennenteelfoundation.org/wp-content/uploads/NASFM-Test-Report-1.pdf [accessed April 2026].

[17] NFPA 70 (National Electrical Code), Article 800: Communications circuits. National Fire Protection Association, Quincy, MA. 2023.

[18] RTCA DO-160G. Environmental conditions and test procedures for airborne equipment. Section 22: Lightning induced transient susceptibility. RTCA, Inc., Washington, DC. 2010.

[19] IEC 61000-4-5. Electromagnetic Compatibility (EMC) — Part 4-5: Testing and measurement techniques — surge immunity test. International Electrotechnical Commission. Edition 3.0, 2014.

[20] IEC 61511. Functional safety — safety instrumented systems for the process industry sector. International Electrotechnical Commission. 2016.

[21] Maxwell JC. A dynamical theory of the electromagnetic field. Philos Trans R Soc Lond. 1865;155:459–512.

[22] Griffiths DJ. Introduction to Electrodynamics. 4th ed. Cambridge: Cambridge University Press; 2017. pp. 65–70, 96–98.

[23] Faraday M. Experimental researches in electricity. Philos Trans R Soc Lond. 1838.

[24] Deblois DA, Zeik TP, Baker SM. Test report: high current arc entry testing on CSST gas tubing samples using LC1027 & LC1024 methods. Lightning Technologies, Pittsfield, MA; 2013. Available from: https://csstdanger.com/wp-content/uploads/2013/04/LT-13-36912.pdf [accessed April 2026].

[25] Zeik TP, Saldo PP, Crochiere GA. Test report: CSST gas pipe lightning high voltage and high current characterization tests and model validation tests. In: Hammerschmidt A, Ziolkowski CJ, editors. GTI CSST final report (amended 9-5-13), Appendix C. Gas Technology Institute; 2013.

[26] Spruiell JP, Hergenrether MC, Colwell CK. Lightning-caused CSST hole formation with concurrent ignition of escaping fuel gas: validation of field observations by laboratory testing. In: Proceedings of the International Symposium on Fire Investigation Science and Technology (ISFI). International Association of Arson Investigators; 2014.

[27] Rousseau A. Validation of installation methods for CSST gas piping to mitigate lightning related damage: Phase 1 final report. Report No. X54 Part3 V1. Fire Protection Research Foundation, Quincy, MA. Project Contractor: SEFTIM, Vincennes, France; 2011.

[28] Rakov VA, Uman MA. Lightning: Physics and Effects. New York: Cambridge University Press; 2003.

[29] Insurance Information Institute. Facts + Statistics: Homeowners and renters insurance. ISO, a Verisk Analytics business; 2025. Available from: https://www.iii.org/fact-statistic/facts-statistics-homeowners-and-renters-insurance [accessed April 2026].

[30] Revie RW, editor. Uhlig's Corrosion Handbook. 3rd ed. Hoboken, NJ: Wiley; 2011. pp. 35–60.

[31] U.S. Department of Defense. Galvanic Compatibility of Electrically Conductive Materials, MIL-STD-889D. Washington, DC; 2021. Available from: https://corrdesa.com/wp-content/uploads/2024/04/MIL-STD-889D-2021-Release.pdf [accessed April 2026].

[32] Frank R, Morton C. Comparative corrosion and current burst testing of copper and aluminum electrical power connectors. IEEE Industry Applications Conference; 2005. Available from: https://copper.org/applications/electrical/building/pdf/A6108.pdf

[33] Lall P, Luo Y, Nguyen L. Multiphysics-modeling of corrosion in copper-aluminum interconnects in high humidity environments. 2015 IEEE 65th Electronic Components and Technology Conference (ECTC), San Diego, CA, USA; 2015. pp. 1045–1056. https://doi.org/10.1109/ECTC.2015.7159724

[34] Bauer B. F-connector corrosion in aggressive environments — an electrochemical and practical evaluation. 1991 NCTA Technical Papers; 1991. pp. 25–35. Available from: https://nctatechnicalpapers.com/wp-content/uploads/2025/09/1991-f-connector-corrosion-in-aggressive-environments-an-electrochemical-and-practical-evaluation.pdf

[35] Gao C, Wang L, Wu S, Xie C, Liu L, Li E, et al. Increase in the visual corona from floating electrodes. J Electrostat. 1999;46(1):1–15. https://doi.org/10.1016/S0304-3886(98)00047-3

[36] Gao J, Wang L, Wu S, et al. Effect of a floating conductor on discharge characteristics of a long air gap under switching impulse. J Electrostat. 2021;114:103629. https://doi.org/10.1016/j.elstat.2021.103629

[37] Wu S, Wang L, Gao J, Xie C, Liu L, Wang T, et al. Breakdown characteristics of combined air gaps under lightning impulse. AIP Advances. 2022;12(3):035024. https://doi.org/10.1063/5.0084951

[38] Xie C, Wang L, Gao J, et al. Prediction method of breakdown voltage of long air gaps containing a floating conductor. Electr Eng. 2022;104:4169–4177. https://doi.org/10.1007/s00202-022-01605-5

[39] Zhang Z, Zhu Z, Zeng D, Jiang X, Yang B, Liu H, et al. Lightning impulse breakdown voltage correction based on discharge characteristic detection of different long electrode air gaps at 1450 m a.s.l. Electr Power Syst Res. 2026;236:112709. https://doi.org/10.1016/j.epsr.2026.112709

[40] Kim DJ, et al. Corona discharge behaviors with presence of floating electrode in air insulation using numerical model analysis. J Mater Sci Manuf Res. 2023. https://doi.org/10.47363/JMSMR/2023(4)144

[41] Tran MD, Rakov VA. A study of the ground-attachment process in natural lightning with emphasis on its breakthrough phase. Sci Rep. 2017;7:15761. https://doi.org/10.1038/s41598-017-14842-7

[42] Cummins KL, Krider EP, Olbinski M, Holle RL. A case study of lightning attachment to flat ground showing multiple unconnected upward leaders. Atmos Res. 2018;202:169–174. https://doi.org/10.1016/j.atmosres.2017.11.007

[43] Cooray V, Jayasinghe H, Rubinstein M, Rachidi F. The geometry and charge of the streamer bursts generated by lightning rods under the influence of high electric fields. Atmosphere. 2022;13(12):2028. https://doi.org/10.3390/atmos13122028

[44] Schumann C, Saba MMF, Warner TA, Ferro MAS, Helsdon JH, Thomas R, et al. On the triggering mechanisms of upward lightning. Sci Rep. 2019;9:9576. https://doi.org/10.1038/s41598-019-46122-x

[45] Vukovic F, Milardic V, Filipovic-Grcic B, Stipetic N. Electromagnetic transients and failed upward leaders observed during lightning activity in an onshore wind farm. Electr Power Syst Res. 2025;238:111031. https://doi.org/10.1016/j.epsr.2025.111031

[46] Alipio R, Guimarães M, Passos L, Conceição D, Correia de Barros MT. Ground potential rise in wind farms due to direct lightning. Electr Power Syst Res. 2021;194:107110. https://doi.org/10.1016/j.epsr.2021.107110

[47] Bazelyan EM, Raizer YuP, Aleksandrov NL. Non-stationary corona around multi-point system in atmospheric electric field: I. Onset electric field and discharge current. J Atmos Sol-Terr Phys. 2014;109:80–90. https://doi.org/10.1016/j.jastp.2013.03.029

[48] IEC 60060-1. High-voltage test techniques — Part 1: General definitions and test requirements. International Electrotechnical Commission. Edition 3.0, 2010.

[49] Friedman S. Experts say flexible gas line lightning-related fires continue in spite of new safety measures. NBC 5 Dallas-Fort Worth; 2014. Available from: https://www.nbcdfw.com/news/local/experts-say-flexible-gas-line-lightning-related-fires-continue-in-spite-of-new-safety-measures/188585/ [accessed April 2026].

[50] Karthikeyan R. Appendix A. Action Integral Calculations for Retrofit Electromagnetic Shielding of CSST to Mitigate Fires from Lightning Transients, AC Fault Currents, and Ground Potential Rise. Zenodo; 2026. https://doi.org/10.5281/zenodo.19582338